Asian Journal of Chemistry; Vol. 27, No. 9 (2015), 3420-3430

ASIAN JOURNAL OF CHEMISTRY

http://dx.doi.org/10.14233/ajchem.2015.18904

Removal of Cr(III) and Cr(VI) from Aqueous Solution by Biosorption Using Agricultural Waste Materials: Batch and Continuous Reactor Study

PRANAB JYOTI SARMA[1,2,†], RAJNEESH KUMAR[1,2,†], N. ARUL MANIKANDAN[3] and KANNAN PAKSHIRAJAN[1,3,*]

[1]Centre for the Environment, Indian Institute of Technology Guwahati, Guwahati-781 039, India
[2]National Institute of Foundry and Forge Technology, Ranchi-834 003, India
[3]Department of Biosciences and Bioengineering, Indian Institute of Technology Guwahati, Guwahati-781 039, India

*Corresponding author: Fax: +91 361 2690762; Tel: +91 361 2582210; E-mail: pakshi@iitg.ernet.in
†These authors contributed equally to this work.

Received: 4 December 2014; *Accepted*: 5 January 2015; *Published online*: 26 May 2015; AJC-17269

In this study, different agricultural waste materials, namely rice husk, sugarcane bagasse, mustard oil cake, tea waste, betel nut peel and saw dust, were investigated for their potential to remove Cr(III) and Cr(VI) from aqueous solutions. The effect of solution pH, contact time, biosorbent dosage and initial Cr(III)/Cr(VI) concentration on its biosorption was first studied under batch condition. Among the six biosorbents tested in this study, sugarcane bagasse removed Cr(III) with a maximum efficiency of 89.14 %, whereas rice husk yielded a maximum Cr(VI) removal efficiency of 79.48 % under the batch condition. Chromium sorption kinetics was best explained by the intra particle diffusion based second order kinetics model. Fourier transform infrared, scanning electron microscope analyses of sugarcane bagasse and rice husk were performed before and after its chromium loading in order to analyze the morphology and the functional groups responsible for the chromium biosorption. Continuous column sorption of Cr(III) and Cr(VI) were carried out in two identical fixed-bed columns with sugarcane bagasse and rice husk, respectively, as the biosorbents. The influence of bed depth and flow rate on continuous chromium sorption was investigated at 30 mg L^{-1} inlet concentration. The chromium breakthrough and saturation time in both the columns increased with a decrease in the flow rate from 30 to 10 mL min^{-1}. The same effect was observed with an increase in the column bed depth from 10 to 30 cm.

Keywords: Biosorption, Chromium, Agricultural waste material, Fixed-bed column, Breakthrough curve.

INTRODUCTION

Heavy metals are used extensively worldwide for various industrial applications. This has resulted in the discharge of heavy metal containing wastewater into the environment. Among the different heavy metals, chromium and its salts have many industrial uses, such as in the tannery, electroplating, metal processing, wood preservative, paint and pigments, textile, dyeing, steel fabrication, canning industry, *etc*.[1]. Chromium exists in natural water in two main oxidation states *i.e.*, hexavalent chromium [Cr(VI)] and trivalent chromium [Cr(III)]. Chromium(VI) is more hazardous, carcinogenic and mutagenic to living organisms[2]. The permissible levels of Cr(VI) in potable water, inland surface water and industrial wastewater, as specified by the World Health Organization (WHO) are 0.05, 0.1 and 0.25 mg L^{-1}, respectively[3].

Therefore, it is necessary to eliminate chromium from discharge wastewater entering the environment. In general, chromium is removed from wastewater by various methods, such as chemical precipitation, electrochemical reduction, sulphide precipitation, ion exchange, reverse osmosis, electrodialysis, solvent extraction and evaporation. All these methods suffer from one or more drawbacks, such as high cost, inefficient chromium removal, *etc*. Compared to these methods, biosorption using plants, microbes or any other kind of biomass seems more attractive due to the ability of this biomass to bind strongly to chromium and high loading capacity[4].

Although several studies have been conducted to examine chromium removal from wastewater by biosorption, most of these studies have either been carried out using specially prepared biosorbents or limited only to batch shake flasks. In order that the biosorption process is economical, the biosorbent should be based on locally available low-cost waste materials, such as those from the agricultural industry.

Although several types of plant and microbial biomass have been screened and studied for chromium removal (Table-1), the search for low-cost and abundantly available biosorbent materials still continues to allow cheap large-scale applications

TABLE-1
MAXIMUM CHROMIUM SORPTION CAPACITY OF SELECTED ALGAL, PLANT OR FRUIT WASTE-BASED BIOSORBENTS[a]

Biosorbent	Uptake capacity (mg/g)	References
Cr(III)		
Sugarcane bagasse	24.05	This study
Palmaria palmate	29.63	5
Sargassum wightii	13.00	6
Ulva lactuca	36.91	5
Rhizoclonium hieroglyphicum	11.81	7
Spirogyra condensate	14.82	8
Spirogyra spp	28.16	9
Ceramium virgatum	26.50	10
Eckonia sp	20.50	11
Cr(VI)		
Pine leaves dried biomass of cyanobacterium	0.198	12
Sawdust	0.470	12
Raw and modified palm branches	55.0	13
Oscillatoria laetevirens	103.09	14
Diatom: *Planothidium lanceolatum*	93.45	15
Biomass of *Trichoderma gamsii*	44.8	16
Dead biomass of green algae *Spirogyra* spp.	265.0	17
Tea fungus	58.0	18
Trametes versicolor Polyporus fungi	125.0	19
Rice husk powder	21.82	Present study

in low income countries. This study was, therefore, aimed at developing low-cost and easily available agricultural waste, *viz*., rice husk, sugarcane bagasse, betel nut peels, sawdust, tea waste and mustard oil cake, to remove Cr(III) and Cr(VI) from syn-thetic wastewater. The influence of pH, contact time, biomass dosage and initial metal concentration on biosorption was first investigated under batch condition. Dynamic column experiments were then carried out to remove Cr(III) and Cr(VI) under continuous condition. Besides, characterization of these biosorbents using Fourier transform infrared (FTIR) spectroscopy and scanning electron microscopy (SEM) techniques was carried out.

EXPERIMENTAL

Source and preparation of biosorbents: Agricultural waste materials used in this study were rice husk, sugarcane bagasse, mustard oil cake, tea waste, betel nut peels and saw dust; these materials were collected from Gandhiya Village, Nalbari (near Guwahati), Assam, India. These materials were cut into small pieces followed by washing with tap water to remove unwanted impurities. They were further washed with distilled water to remove any water soluble impurities and other surface adhered particles. The materials were then dried in a hot air oven for 24 h at 60-70 ºC, crushed with a mixer grinder and finally, sieved to obtain uniform size in the range 0.3-0.7 mm. These materials were subsequently used in the biosorption experiments.

Batch biosorption experiment: Stock solution each of Cr(III) and Cr(VI) (1000 mg L^{-1} concentration) was prepared by dissolving an accurate quantity of chromium nitrate [$Cr(NO_3)_3 \cdot 9H_2O$] and potassium chromate, respectively, in 1000 mL of distilled water. These stock solutions were diluted as necessary for preparing chromium containing solution for the biosorption experiments. Batch experiments were carried out using 250 mL Erlenmeyer flasks with 50 mL Cr(III)/Cr(VI) containing solution. To these flasks containing 50 mg L^{-1} of Cr(III)/Cr(VI) solution, a specific amount of the biosorbents (20 g L^{-1}) was added individually. The flasks were then kept at 25 ºC in an orbital incubator shaker at 150 rpm with the solution pH unadjusted for this study. Samples were withdrawn at specific time intervals, filtered using a Whatmann Filter paper and analyzed for the residual Cr(III)/Cr(VI) concentration in solution. Results were expressed as either % chromium removal or sorption capacity (q, mg chromium removed per gram of biosorbent) as given in eqns. 1 and 2, respectively:

$$\text{Chromium removal}\,(\%) = \frac{(C_i - C_e)}{c_i} \times 100 \quad (1)$$

$$q = \frac{V(C_i - C_e)}{m} \quad (2)$$

where, C_i and C_e are initial and final concentration of chromium in solution (mg L^{-1}), respectively, q is the chromium uptake/sorption capacity (mg g^{-1} of biomass), V is the volume of chromium containing solution (L) and m is the biosorbent dry weight (g).

Influence of process parameters on chromium biosorption: The effect of various parameters, *viz*., solution pH, biosorbent dose and initial chromium concentration, on Cr(III)/Cr(VI) removal by the different biosorbents were studied. The effect of solution pH on chromium removal was studied by varying the initial pH of the solution from 2 to 7 with 50 mg L^{-1} initial chromium concentration and 20 g L^{-1} of the individual biosorbents. The effect of biosorbent dose on chromium biosorption was studied in the range 5-20 g L^{-1} with 50 mg L^{-1} initial chromium concentration and its solution pH was adjusted to an optimum value for Cr(III) and Cr(VI) based on the previous experiment. To study the effect of initial Cr(III) and Cr(VI) concentration on their biosorption, the concentration range chosen was 25-500 mg L^{-1} at a pH optimum for each of the metals. All these experiments were carried out using 250 mL Erlenmeyer flasks with 50 mL working volume.

Chromium sorption isotherm: In order to evaluate the capacity of the different biosorbents to sequester Cr(III)/Cr(VI) from aqueous solution, the sorption isotherm data obtained using different initial Cr(III)/Cr(VI) concentration, ranging from 25 to 500 mg L^{-1} was fitted to various isotherm models reported in the literature. These models are presented in Table-2.

Chromium sorption kinetics: To determine the kinetics of Cr(III) and Cr(VI) sorption using the different biosorbents, experimental data was fitted to the pseudo first-order and second-order kinetic models reported in the literature. These models are briefly discussed further.

The first-order rate kinetics of chromium uptake by the biosorbents was expressed as follows[23]:

$$\frac{dq_t}{dt} = k_1(q_e - q_t) \quad (7)$$

TABLE-2
ISOTHERM MODELS TESTED IN THE BATCH STUDY FOR CHROMIUM BIOSORPTION

Isotherm	Equation	Equation No.	Plot	Estimable parameters	Reference
Langmuir	$q_e = \frac{q_{max} b C_e}{1 + b C_e}$	(3)	C_e/q_e *vs.* C_e and q_e *vs.* C_e	q_{max}, b	20
Freundlich	$q_e = K_F C_e^{1/n}$	(4)	log q_e *vs.* log C_e	K_F, η	20
Sips	$q_e = \frac{q'_{max} b C_e^{1/n}}{1 + b C_e^{1/n}}$	(5)	q_e *vs.* C_e	q'_{max}, b, η	21
Redlich- Peterson	$q_e = \frac{K_{RP} C_e}{1 + \alpha_{RP} C_e^{\beta}}$	(6)	q_e *vs.* C_e	K_{RP}, α_{RP}, β	22

$$\ln(q_e - q_t) = \ln q_e - k_1 t \quad (8)$$

where k_1 is the Lagergren first order rate constant (min^{-1}), q_e and q_t are the sorption capacity (mg g^{-1}), respectively and t is the time (min). A plot of log (q_e-q_t) *versus* t presents a linear relationship from which values of k_1 and q_e are obtained from the slope and intercept of the line, respectively.

The pseudo second-order model is based on the assumption that the rate-limiting step is chemical sorption or chemisorption involving valence forces through sharing or exchange of electrons between sorbent and sorbate as covalent forces[24]. Mathematically, it is expressed as:

$$\frac{dq_t}{dt} = k_2 (q_e - q_t)^2 \quad (9)$$

$$\frac{t}{q_t} = \frac{1}{k_2 q_e^2} + \frac{1}{q_e} t \quad (10)$$

$$\frac{t}{q_t} = \frac{1}{h} + \frac{1}{q_e} \quad (11)$$

where k_2 (g mg^{-1} min^{-1}) is the second-order rate constant, q_e (mg g^{-1}) is the maximum sorption capacity, q_t (mg g^{-1}) is the amount adsorbed at time t (min). The product $k_2 q_e^2$ is the initial sorption rate represented as $h = k_2 q_e^2$. Eqn. 11 is the linear form of the pseudo second-order equation.

Biosorbent characterization: Morphological analysis of the biosorbents (sugarcane molasses and rice husk), before and after Cr(III)/Cr(VI) biosorption was carried out using a scanning electron microscope (SEM) (LEO 1430VP, Japan); its qualitative elemental constitution responsible for the metal uptake was analyzed by energy dispersive X-ray (EDX) analysis coupled to the SEM.

The functional groups responsible for chromium sorption by the biosorbents were identified using Fourier transform infrared spectroscopy (FTIR) (Spectrum One, Perkin Elmer, USA). The weight ratio of the biomass sample to potassium bromide taken for this analysis was 1:100. Prior to the analysis, samples were compacted into thin pellets[25].

Dynamic column experiment

Experimental setup: Continuous chromium biosorption experiments were conducted using two identical columns of Perspex material with 2 cm diameter and 30 cm length each. One of the columns was packed with sugarcane bagasse for Cr(III) biosorption and the other was packed with rice husk for Cr(VI) biosorption. These biosorbents were supported by layers of pre-equilibrated glass wool at both ends in each of the columns. Suitable sample ports were provided at 10, 20 and 30 cm along the height of the column as shown in the column setup (Fig. 1).

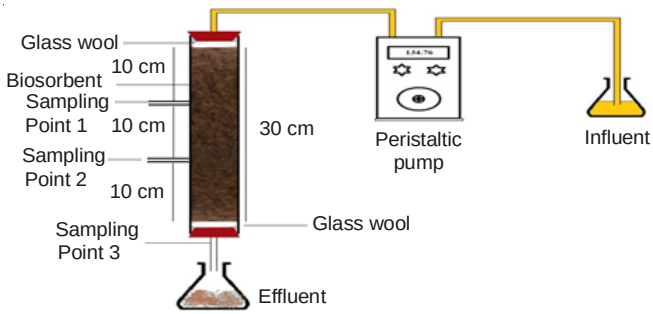

Fig. 1. Schematic of the fixed-bed column setup used in the continuous biosorption experiments

Effect of flow rate and column bed depth: To study the effect of flow rate and column bed depth on Cr(III) and Cr(VI) biosorption in their respective columns, experiments were conducted at room temperature with an initial chromium concentration of 30 mg L^{-1}. Whereas the different bed depths investigated in each column were 10, 20 and 30 cm, the effect of flow rate was investigated in the range 10-30 mL min^{-1}. The biosorbent amount corresponding to these bed heights were 11.2, 22.5 and 33.7 g, respectively, in case of sugarcane bagasse; whereas, in case of rice husk, these values were 9.26, 18.5 and 27.8 g, respectively. The initial solution pH was 4 and 3 for Cr(III) and Cr(VI), respectively, which were found optimum from the batch sorption experiments. Samples were collected at regular time intervals from the column exit and were analyzed for chromium concentration. All these dynamic column experiments were continued until column saturation with the metal, *i.e.*, until when the chromium concentration in the influent and the effluent remained unchanged[3].

Column data analysis: The column data in the study was analyzed in the form of time and shape of the breakthrough curve, which were obtained by plotting C_e/C_i *vs.* time for different conditions of flow rate and bed depth, where C_e and C_i are the effluent and inlet chromium concentrations, respectively.

The effluent volume, (V_{eff}, mL), collected was calculated through eqn. 12:

$$V_{eff} = Q\, t_{total} \quad (12)$$

where t_{total} is total time in min and Q is flow rate through the column in mL min^{-1}.

The area under the breakthrough curve represents the total mass of chromium adsorbed, (q_{total}, mg). For a given feed concentration and flow rate, it was determined using eqn. 13:

$$q_{total} = \frac{Q}{1000}\int_{t=o}^{t_{total}} C_{ad}\,dt \qquad (13)$$

where $C_{ad} = C_i - C_e$ is the concentration of chromium adsorbed in mg L^{-1}.

The equilibrium uptake ($q_{e(exp)}$), *i.e.*, the amount of chromium sorbed (mg) per unit dry weight of biosorbent (mg g^{-1}) in the column was calculated using eqn. 14:

$$q_e = \frac{q_{total}}{m} \qquad (14)$$

where m is the total dry weight (g) of biosorbent in the column.

Analytical methods: All chemicals used for preparing chromium standards and reagent solutions for analysis of chromium were of analytical grade and deionized water was used in preparing the metal containing solutions. For chromium analysis the diphenyl carbazide method[8] was followed. The concentration of Cr(III) and Cr(VI) were determined from a calibration curve prepared using the respective standard solutions and their absorbance read at 540 nm using a UV-visible spectrophotometer (Cary 100,Varian, Australia).

RESULTS AND DISCUSSION

Effect of batch process parameters on chromium biosorption

Contact time: Chromium biosorption by the different biosorbents occurred within the first five min and gradually increased up to 3 h [Fig. 2(a)]. Sugarcane bagasse showed maximum Cr(III) removal efficiency of 89.8 % within 3 h. Chromium(III) removal efficiency using the other biosorbents was in the following order: betel nut peels (67.1 %) > rice husk (63.1 %) > mustard oil cake (59.8 %) > tea waste (57.2 %) > sawdust (28.1 %). The Cr(III) sorption reached equilibrium with each biosorbent at about 3 h of contact time. Similarly, highest % Cr(VI) removal took place in the first 5 min and equilibrium was established at about 3 h. However, for Cr(VI) removal, tea waste showed a maximum removal efficiency of 69.4 % followed by other biosorbents, which were in the order: sugarcane bagasse (52.3 %) > sawdust (52.2 %) > rice husk (52.1 %) > mustard oil cake (42.7 %) > betel nut (37.8 %). Thus Fig. 2(a) showed that the chromium biosorption increased with an increase in the contact time. The initial rapid rate of biosorption is attributed to the availability of the positively charged surface of the biosorbents. The later slow biosorption rate may be due to the electrostatic hindrance caused by the already sorbed negatively charged chromium species and the slow pore diffusion of the chromium ions[26].

Solution pH: Chromium(III) biosorption depended strongly upon the solution pH; its uptake increased with a decrease in the solution pH [Fig. 2(b)]. Maximum Cr(III) removal was observed with sugarcane bagasse (89.1 %) at pH 4. At other pH values, Cr(III) removal efficiency by the biosorbent was minimum [Fig. 2(b)]. Similar observations on Cr(III) removal using the other biosorbents was made. Its order of removal among the other biosorbents based on optimum pH was: betel nut peel (79.7 % at pH 3) > rice husk (72.6 %

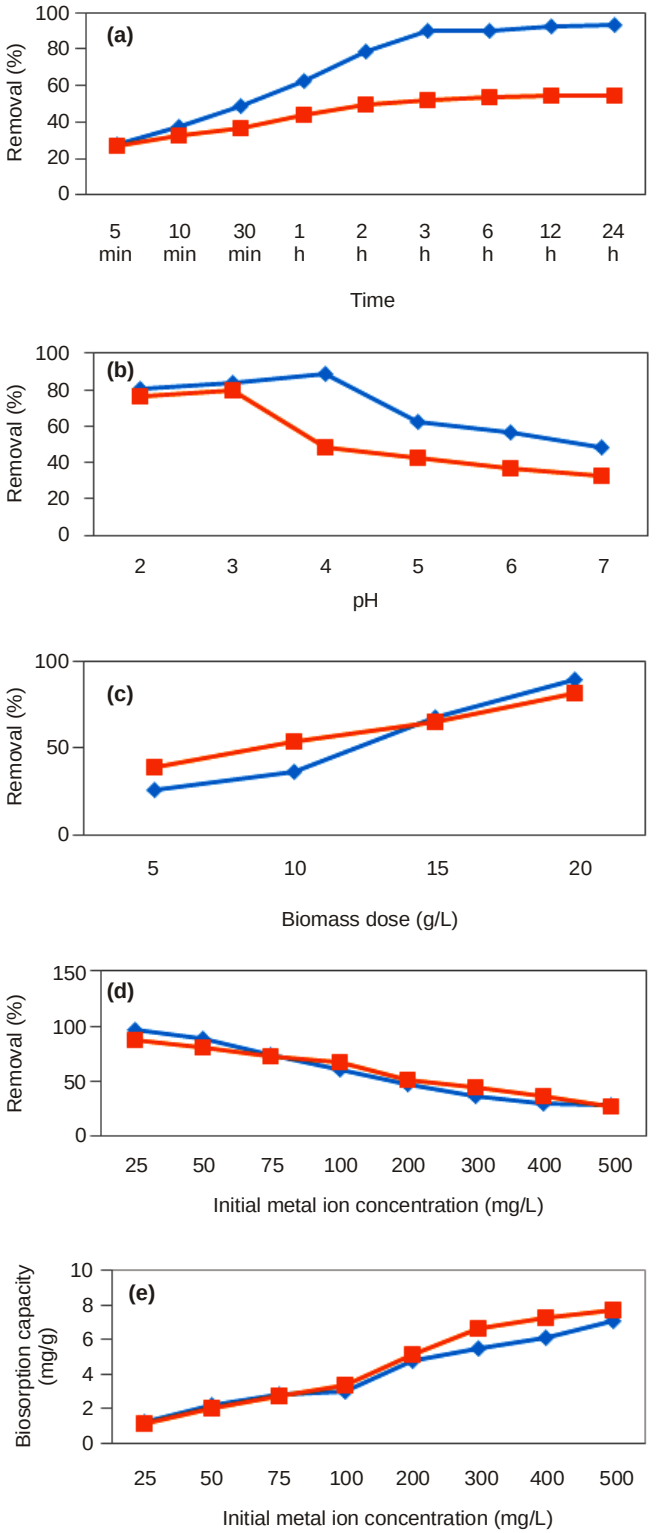

Fig. 2. Effect of different process parameters on the batch removal of Cr(III) using sugarcane bagasse (◆) and Cr(VI) using rice husk (■) as the biosorbent: (a) contact time (temperature = 25 ºC, shaking speed = 150 rpm, initial chromium concentration= 50 mg L^{-1}, biomass dose = 20 g L^{-1}, unadjusted pH), (b) pH (temperature = 25 ºC, shaking speed = 150 rpm, initial chromium concentration = 50 mg L^{-1}, biomass dose = 20 g L^{-1}), (c) biomass dose (temperature = 25 ºC, shaking speed = 150 rpm, initial chromium concentration = 50 mg L^{-1}, pH = 4.0 for sugarcane bagasse and pH 3.0 for rice husk), (d) initial chromium concentration (temperature = 25 ºC, shaking speed = 150 rpm, pH = 4.0 for sugarcane bagasse and pH 3.0 for rice husk) and (e) sorption capacity *versus* initial chromium concentration

at pH 4) > mustard oil cake (62.2 % at pH 4) > tea waste (61.3 % at pH 4) > sawdust (43.4 % at pH 3). In case of Cr(VI) removal, a maximum removal efficiency of 79.8 % was obtained using rice husk at pH 3 and the efficiency decreased with an increase in the pH from 4 to7 [Fig. 2(b)]. For the other biosorbents, it followed the order: tea waste (77.5 % at pH 2) > sugarcane bagasse (74.2 % at pH 3) > mustard oil cake (67.6 % at pH 2) > sawdust (62.3 % at pH 3) > betel nut peel (57.4 % at pH 2). Thus, pH of the solution was found to be the most vital among all the parameter for chromium biosorption. Chromium uptake increased with a decrease in the solution pH [Fig. 2(b)]. Cr(III) precipitates in the form of $Cr(OH)_3$ at near-neutral pH values. Also, it is well known that Cr(III) in water undergoes hydrolysis depending on the total Cr(III) concentration, the pH and the type of anions present in the solution. The Cr(III) hydrolysis can be represented as follows:

$$Cr^{3+} + H_2O \rightleftharpoons Cr(OH)_2^+ + H^+ \quad (15)$$

The above reaction generates $Cr(OH)_2^+$ and protons which contribute to the reduction in the pH of Cr(III) solution. In addition, a low pH value also affects the ionic state of the functional groups in the biosorbent involved in the chromium binding.

Chromium(VI) is easily hydrolyzed in water and at low pH values $HCrO_4^-$ is the predominant species; decrease in pH further leads to the formation of different oxidized chromium species such as CrO_4^{2-} as indicated further.

$$HCrO_4^- \rightleftharpoons H^+ + CrO_4^{2-} \quad (16)$$

Thus, a decrease in pH causes formation of more positively charged sorbent surface to bind all the negatively charged Cr(VI) species. As the pH increased, the H^+ concentration decreases and the surface charge of the sorbent becomes negative, thereby causing a reduction in Cr(VI) retention onto its surface[27].

Biosorbent dose: Chromium removal efficiency increased with an increase in the biosorbent dose for all the biomass materials [Fig. 2(c)], but its sorption capacity decreased with the dose. A maximum Cr(III) removal of 89 % was obtained using sugarcane bagasse at 20 g L^{-1}; whereas, at 15 g L^{-1}, the removal was only 67 % [Fig. 2(c)]. In the case of other biosorbents, the removal was low and the order followed was: betel nut peel > rice husk > mustard oil cake > tea waste > sawdust. Similarly, rice husk yielded the highest Cr(VI) removal at 20 g L^{-1}, which was followed by the other biosorbents in the order: tea waste > sugarcane bagasse > mustard oil cake > sawdust > betel nut peel. At 5 g L^{-1} biomass dose, the chromium removal was very low for all these biosorbents, but it gradually increased with an increase in the dose. Thus maximum removal of Cr(III)/Cr(VI) was obtained at 20 g L^{-1} dose of these biosorbents. Chromium sorption capacity was dependent on biosorbent dose [Fig. 2(c)], which is attributed to the availability of more surface area for sorption with an increase in the biosorbent dose[28].

Initial chromium concentration: A maximum Cr(III) removal of 96.21 % was shown by sugarcane bagasse at 25 mg L^{-1} initial concentration [Fig. 2(d)]. At the same concentration, its removal by other biosorbents was low and followed the order: rice husk > betel nut peel > mustard oil cake > tea waste > sawdust. In case of Cr(VI) removal, the maximum removal obtained was 87.3 % using rice husk at 25 mg L^{-1} initial concentration. With the other biosorbents, the removal was low and followed the order: tea waste > sugarcane bagasse > mustard oil cake > sawdust > betel nut. In general, chromium biosorption was maximum at 25 mg L^{-1} initial concentration and was lower at 500 mg L^{-1} initial concentration for these biosorbents [Fig. 2(d)]. On the other hand, Cr(III)/Cr(VI) sorption capacity of the biosorbents increased with an increase in the initial metal ion concentration. Thus, the chromium removal efficiency increased with an increase in initial chromium concentration in solution [Fig. 2(d)]. At a lower concentration, chromium ions in solution interact with the binding sites on the biosorbents, thus facilitating maximum sorption. At higher concentrations, due to the saturation of the binding sites not all chromium ions are removed from the solution. Hence, percentage removal of Cr(III) decreased with an increase in initial chromium concentration.

Chromium sorption isotherm modelling: Experimental chromium sorption isotherm data obtained using the different biosorbents and at different initial Cr(III)/Cr(VI) concentration was fitted to the Langmuir, Freundlich, SIPS and Redlich-Peterson models. The maximum sorption capacity and other parameters estimated from these models are presented in Table-3. The Langmuir model revealed a q_{max} value in the range of 4.6-6.8 mg g^{-1} for Cr(III) and for Cr(VI) it was in the range of 5.4-8.2 mg g^{-1}. The value of the affinity factor b was obtained in the range 0.00473-0.02992 L mg^{-1} for Cr(III) and its value was 0.0119-0.0281 L mg^{-1} for Cr(VI) biosorption. These values of q_{max} and b corresponding to sugarcane bagasse and rice husk for Cr(III) and Cr(VI) biosorption, respectively, were the highest among all the biosorbents tested in this study.

TABLE-3
ESTIMATED SORPTION ISOTHERM MODEL PARAMETERS FOR CHROMIUM BIOSORPTION IN THE BATCH STUDY

Model	Parameters	Cr(III) with sugarcane bagasse	Cr(VI) with rice husk
Langmuir (non-linear)	q_{max} (mg g^{-1})	6.8	7.6
	b (L mg^{-1})	0.02992	0.02816
	R^2	0.860	0.970
Langmuir (linear)	q_{max} (mg g^{-1})	7.0	7.4
	b (L mg^{-1})	0.03156	0.03441
	R^2	0.972	0.990
Freundlich	K_f (L g^{-1})	172.12	52.0
	1/n	0.28495	0.39491
	R^2	0.983	0.973
SIPS	q'_{max} (mg g^{-1})	3.37	16.7
	b (L mg^{-1})	0.04673	0.93508
	n'	2.15	1.85
	R^2	0.985	0.996
Redlich-Peterson	K_{RP} (L mg^{-1})	13.3	17.6
	a_{RP} (L g^{-1})	0.00084	0.00032
	β	0.70868	0.60553
	R^2	0.985	0.993

Compared with the Langmuir model, the Freundlich isotherm model yielded a better fit to the data, in which case

the R^2 value was the highest for Cr(III) using sugarcane bagasse (0.98); a similar high value was obtained for Cr(VI) biosorption using rice husk (0.97) (Table-3). The value of K_F obtained from the Freundlich equation was in the range 3.6–172.12 L g^{-1} for Cr(III) and in case of Cr(VI) it was in the range 15.5-52.0 L g^{-1}. The value of 1/n, which relates the affinity between the different biosorbents and chromium ions, was obtained in the range 0.28-0.52 for Cr(III) and for Cr(VI) it was in the range of 0.39-0.48. These values of 1/n were also high due to sugarcane bagasse and rice husk for Cr(III) and Cr(VI) biosorption, respectively.

By fitting the experimental data using the SIPS model equation, its b value was obtained in the range 0.0011-0.046 L mg^{-1} for Cr(III) using sugarcane bagasse. In case of Cr(VI), it was in the range 0.0022-0.935 L/mg. The value of 1/n was further obtained in the range 1.6-2.4 and 1.6-2.4 for Cr(III) and Cr(VI) biosorption, respectively, using these two biosorbents. The values of b and 1/n obtained were also the highest for sugarcane bagasse and rice husk compared with the other biosorbents for Cr(III)/Cr(VI) biosorption.

The Redlich-Peterson isotherm constant K_R obtained by fitting the experimental data to this model varied in the range 4.9-28.9 L g^{-1} for Cr(III) and 3.7-17.6 L g^{-1} for Cr(VI). Whereas, the value of the model exponent β varied from 0.32 to 0.70 for Cr(III) and in case of Cr(VI) it was in the range 0.53-0.60 for the different biosorbents. The model parameter values obtained due to sugarcane bagasse and rice husk were the highest compared with the other biosorbents.

Chromium biosorption kinetics: The coefficient of determination (R^2) and chromium sorption capacity, ($q_{e\ cal.}$) obtained by fitting the pseudo first-order kinetic model to the experimental data are presented in Table-4. From the R^2 values, it can be clearly seen that the pseudo first-order equation did not provide a good description of Cr (III) or Cr(VI) sorption onto any of the biosorbents.

The experimental data on chromium sorption kinetics was fitted to the pseudo second-order kinetic model. R^2 value of 0.99 obtained due to this model (Table-4) showed its validity in explaining the chromium sorption kinetics by the different biosorbents. The model parameters of k and q_e were further obtained for all the biosorbents tested in this study.

Biosorbent characterization

Fourier transform infrared (FTIR) spectroscopy: The FTIR spectra of sugarcane bagasse and rice husk showed the best removal of Cr(III) and Cr(VI), respectively, were obtained before and after its chromium sorption to determine the functional groups involved in these biosorbents for chromium sorption. These spectra are shown in Fig. 3. The change in the functional groups of the biosorbents due to chromium biosorption is visible from the spectra of the chromium loaded biosorbents which reveals changes in the peaks and wavelength range before and after chromium sorption (Table-5)[29]. The FTIR spectrum (Fig. 3) of the biosorbents further displays a number of absorption peaks, indicating the complex nature of the biosorbent. The broad absorption peak of sugarcane bagasse and rice husk around 3441 and 3466 cm^{-1}, respectively, indicate stretching due to OH and NH, respectively, thus confirming the presence of hydroxyl and amine groups on the biosorbents. The sorption band observed at 1640 and 1685 cm^{-1} can be assigned to mainly the C-O stretch. A band at about 1274 cm^{-1}, representing -CH_2 stretching, was also observed in the FTIR spectrum of sugarcane bagasse but not in the spectrum due to rice husk[29]. Following sorption, the intensity of some of these peaks was either minimized or shifted due to Cr(III)/Cr(VI) loading onto the respective biosorbents. To confirm the difference in functional groups following biosorption of Cr(III) and Cr(VI) by the respective biosorbents, FTIR analysis was carried out with the chromium loaded biosorbents.

Scanning electron microscope (SEM) and energy dispersive X-ray (EDX) spectroscopy: SEM micrographs of the sugarcane bagasse and rice husk showed its porous structure prior to chromium biosorption [Fig. 4(a-c)]. Following chromium biosorption, surface of these biosorbents was found to be highly irregular and rough [Fig. 4(b-d)]. From these images, it is clear that there was significant difference in the surface morphology of these biosorbents before and after chromium sorption. The white clumps seen on the surface of the chromium laden biosorbents were absent in the virgin biomass. The peaks due to calcium, carbon and oxygen indicated the presence of O-H and –COOH functional groups in the biomass[36]. EDX analysis of the biosorbents following chromium biosorption showed

TABLE-4
ESTIMATED KINETIC MODEL PARAMETERS FOR CHROMIUM BIOSORPTION IN THE BATCH STUDY

Biosorbent	$q_{e\ exp}$ (mg/g)	Pseudo first-order kinetic model			Pseudo second-order kinetic model			
		k_1 (min^{-1})	$q_{e\ calc.}$ (mg g^{-1})	R^2	k_2 (g mg^{-1} min^{-1})	h (mg g^{-1} min^{-1})	$q_{e\ calc.}$ (mg g^{-1})	R^2
Chromium(III)								
Rice husk	1.5001	0.0006	0.268904	0.0088	0.119476	0.285323	1.545356	0.9998
Tea waste	1.4305	0.0038	0.922360	0.0450	0.058510	0.134239	1.514693	0.9984
Sugarcane bagasse	2.1145	0.0051	1.000060	0.1849	0.022446	0.118023	2.293052	0.9903
Mustard oil cake	1.4967	0.0021	0.408853	0.0188	0.070013	0.170132	1.558846	0.9992
Betel Nut	1.6780	0.0014	0.797638	0.0558	0.029589	0.086550	1.710279	0.9616
Saw Dust	1.5910	0.0008	0.996705	0.1521	0.033837	0.092567	1.653986	0.9821
Chromium(VI)								
Rice husk	1.98700	0.0037	0.725859	0.0914	0.119476	0.285323	2.039152	0.9971
Tea waste	1.93925	0.0042	0.636672	0.0812	0.058510	0.134239	2.039152	0.998
Sugarcane bagasse	1.85550	0.0025	0.777633	0.0844	0.022446	0.118023	1.936108	0.9865
Mustard oil cake	1.69100	0.0016	0.714409	0.0445	0.070013	0.170132	1.742160	0.9848
Betel Nut	1.43575	0.0023	0.598637	0.0426	0.029589	0.08655	1.534919	0.9961
Saw Dust	1.55925	0.0010	0.788439	0.0386	0.033837	0.092567	1.576790	0.945

TABLE-5
FTIR IN THE RAW BIOSORBENTS AND THEIR SHIFT FOLLOWING CHROMIUM LOADING ALONG WITH THE CORRESPONDING FUNCTIONAL GROUPS

Sugarcane bagasse	Cr(III) loaded sugarcane bagasse	Rice husk	Cr(VI) loaded rice husk	Functional group
3441	3475	3466	3482	NH_2 in aromatic amines
2922	2967	2943	2941	CH_3 and CH_2 in aliphatic compound
2383	2382	–	–	Amine salts
1640	1666	1685	–	Substituted benzene ring
1640	1666	1637	1705	C=O in carboxylic acids
–	–	1637	1623	C=O and NH_2 in primary amides
1397	1382	–	–	COO^- group in carboxylic acid
1274	1274	–	–	AR-O in alkyl ethers
–	–	1110	1161	Hydrated sulphonic acid
1055	1045	1059	–	CH_2-OH in primaryalchols
845	837	–	–	CH-CH_2 in vinyl compounds
–	–	815	–	C-CO-C in ketones

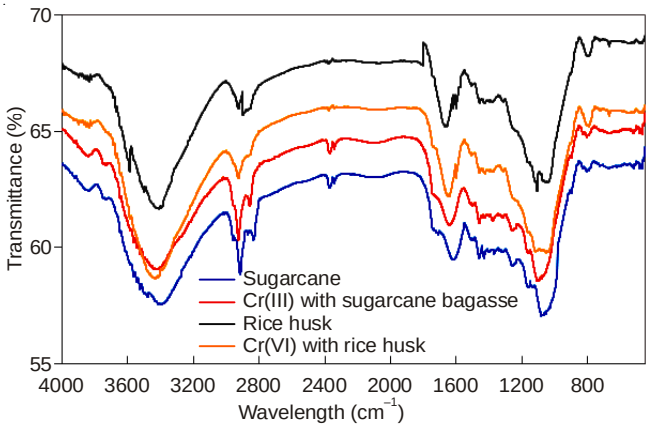

Fig. 3. FTIR spectra of raw and chromium loaded sugarcane bagasse and rice husk

distinct peaks for chromium (Fig. 4), thus providing a direct evidence for chromium biosorption onto the biosorbents.

Continuous chromium biosorption

Effect of bed depth and flow rate: Fig. 5(a) shows the breakthrough curves of Cr(III) biosorption onto sugarcane bagasse and Fig. 5(b) depicts the breakthrough curves of Cr(VI) biosorption onto rice husk. These curves were obtained for different bed depth in the respective columns for an inlet concentration of 30 mg L^{-1} and a constant flow rate of 10 mL min^{-1} in the respective columns. A high uptake of Cr(III) and Cr(VI) was observed at the beginning of the column operation, but their concentration in the effluent rapidly increased following breakthrough. The lower bed depth was saturated with chromium earlier than the higher bed depth in the respective columns. The treated volume, therefore, considerably increased from about 1.38 L to 7.2 L with an increase in the bed depth from 10 to 30 cm (Table-6) for Cr(III); in the case of Cr(VI), it increased from 12.6 L to 16.2 L. Also, an increase in the maximum bed sorption capacity (q_{total}) was noticed at the breakthrough point with an increase in the bed depth**.** Thus, maximum loading capacities of 1697.5, 3792.5 and 6184.8 mg were obtained for Cr (III) for different bed depths (10, 20 and 30 cm) in the column loaded with sugarcane bagasse. In the case of Cr(VI), these values were 2975.3, 4606.8 and 7322.7 mg at 10, 20 and 30 cm bed depth, respectively. Thus, the observed increase in the Cr(III) and Cr(VI) uptake in the respective columns with an increase in the bed depth [Fig. 5(a-b)] can be attributed to an increase in the biosorbent amount available for chromium biosorption. Further, when the bed depth is reduced, axial dispersion predominates in chromium mass transfer, thereby reducing its diffusion onto the biosorbent[31]. Fig. 5(a-b) indicated that an increase in the column bed height enabled the metal ions to better interact with the biosorbent, thereby resulting in an increased uptake of chromium ions. Therefore, an increase in the metal sorption capacity is observed with bed height in the column, which is mainly attributed to an increase in available biosorbent surface area and the number of binding sites[32]. Thus, an increase in the treated volume of chromium containing solution was obtained with delayed breakthrough of chromium ions in the respective columns.

TABLE-6
CHROMIUM UPTAKE CAPACITY OBTAINED IN THE COLUMN STUDY FOR DIFFERENT BED DEPTH AND FLOW RATE

Metal	Bed depth (cm)/ Flow rate (mL min^{-1})	C_o (mg g^{-1})	V_{eff} (mL)	q_{total} (mg)	q_{exp} (mg)	Breakthrough time (min)
Cr(III)	10 cm	30	7800	1697.5	151.5	660
	20 cm	30	10200	3792.5	168.5	1140
	30 cm (Flow rate = 10 mL/min)	30	13800	6184.4	183.5	1320
	20 mL/min	30	10800	1566.7	139.8	480
	30 mL/min (Bed depth = 10 cm)	30	11700	920.7	82.2	330
Cr(VI)	10 cm	30	9600	2975.3	268.5	810
	20 cm	30	12600	4606.8	404.1	1140
	30 cm (Flow rate = 10 mL/min)	30	16200	7322.7	488.8	1500
	20 mL/min	30	11400	1920.9	207.4	570
	30 mL/min (Bed depth = 10 cm)	30	13500	1672.2	180.5	450

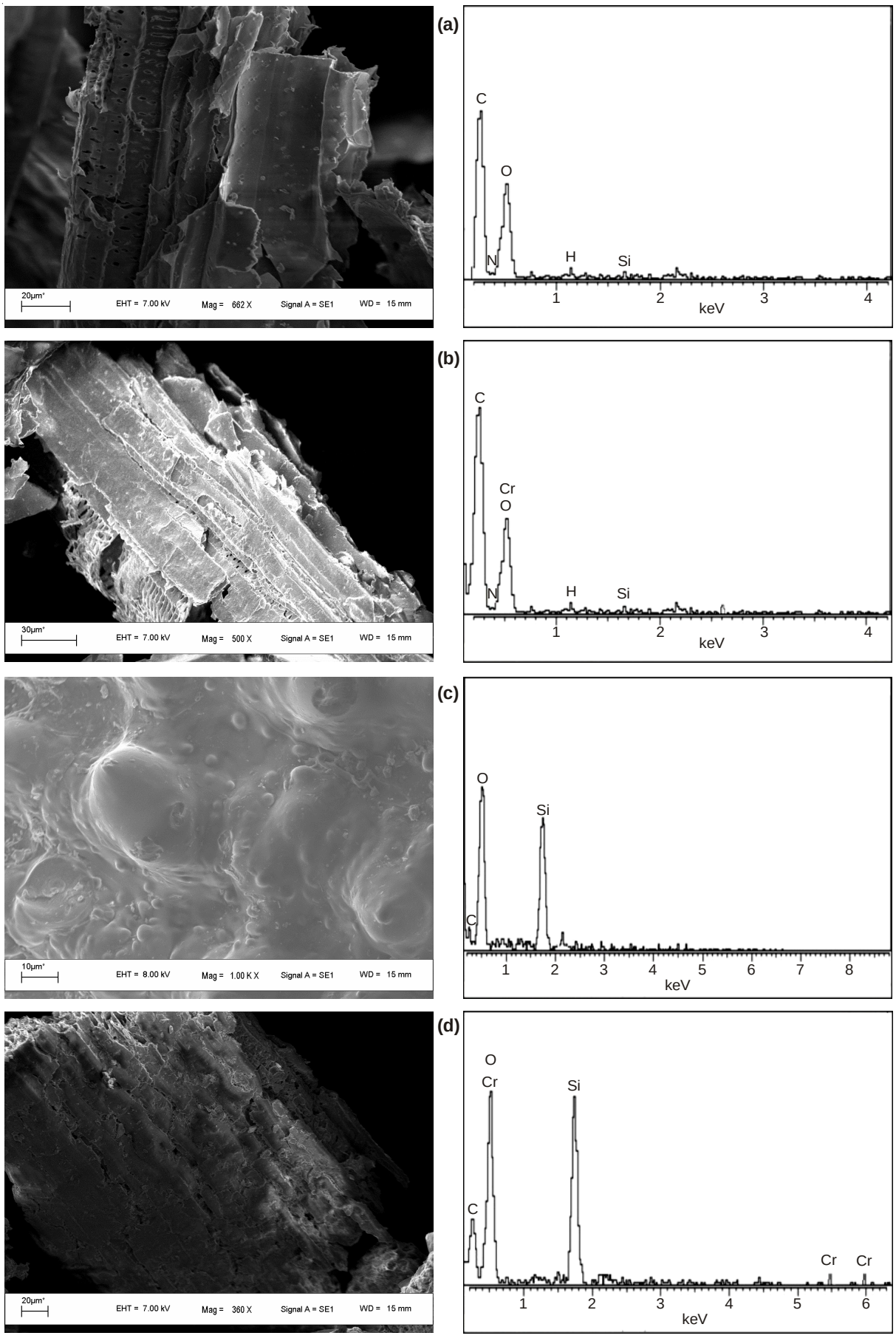

Fig. 4. SEM image and EDX diffractogram of the biosorbents: (a) raw sugarcane bagasse, (b) chromium loaded sugarcane bagasse, (c) raw rice husk and (d) chromium loaded rice husk

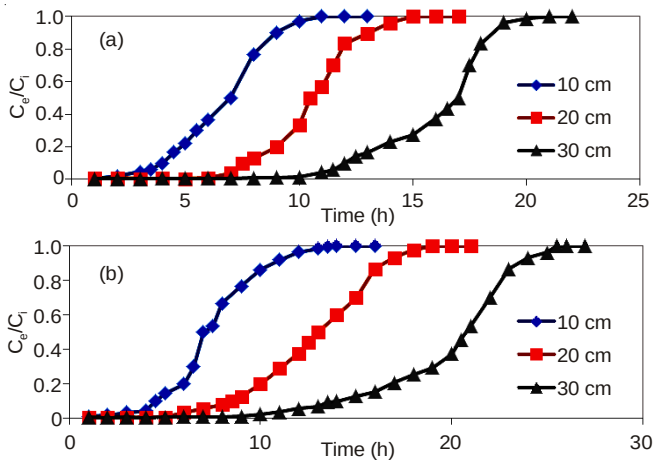

Fig. 5. Effect of bed depth on continuous chromium biosorption in the column study: (a) Cr(III) (inlet solution pH = 4) and (b) Cr(VI) (inlet solution pH = 4). Other conditions: flow rate = 10 mL min^{-1}, inlet chromium concentration (C_o) = 30 mg L^{-1}, particle size = 0.3-0.7 mm, temperature = 25 °C

The effect of flow rate on chromium biosorption in the column study was examined by varying the flow rate from 10 to 30 mL min^{-1}, at a constant bed height of 10 cm and at an initial metal concentration of 30 mg L^{-1} in the respective columns. The breakthrough curves obtained at various flow rates in the respective columns are shown in Fig. 6(a-b). The maximum loading capacity observed was 1697.5, 1566.7 and 920.7 mg for Cr(III) at 10, 20 and 30 mL min^{-1}, respectively; in case of Cr(IV), it was 2975.3, 1920.9 and 1672.2 mg at the same flow rates.

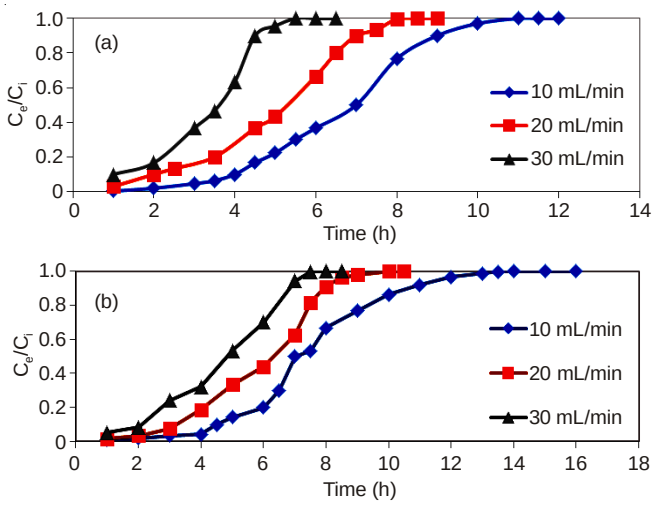

Fig. 6. Effect of flow rate on continuous chromium biosorption in the column study: (a) Cr(III) (inlet solution pH = 4) and (b) Cr(VI) (inlet solution pH = 4). Other conditions: bed height = 10 cm, inlet chromium concentration (C_o) = 30 mg L^{-1}, particle size = 0.3-0.7 mm, temperature = 25 °C.

Breakthrough data modeling: In order to better understand the column behaviour in continuous removal of chromium by the two biosorbents, the experimental breakthrough data was fitted to surface breakthrough models found in the literature. These model equations are given in Table-7 and the results of fitting the experimental breakthrough data to these models are presented in Tables 8 and 9. It could be seen from these tables that among the different models, only the Clark model gave the best fit with the estimated 'r' and 'B' values presented in Table-8. In general, the BDST model is used for the description of the initial part of the breakthrough curve, *i.e.* up to the breakpoint or 10-50 % of saturation limit. Therefore, this model was used for the estimation of maximum chromium sorption capacity and kinetic constant, whose values are presented in Table-9. The Thomas model was applied to the breakthrough data obtained with respect to different bed depth and flow rate in the respective column and from the model parameter presented in the Table-8. It can be seen that the value of the model rate constant with an increase in the bed depth, the k_{Th} (Thomas rate constant) values decreased. On the other hand, with an increase in the flow rate the value of k_{Th} and q_0 increased. The results presented in Table-8 further revealed that the value of the Yoon Nelson's model parameter k_{YN} decreased with an increase in the bed depth. However, its value increased with an increase in the flow rate. On the contrary, a reverse trend is observed for the value of time required for retaining 50 % of the initial adsorbate τ (Table-8). Thus, the chromium breakthrough time was reduced with an increase in the flow rate from 10 to 30 mL min^{-1} [Fig. 6(a-b)]. This can be explained due to the decrease in the residence time of the metal solution in the column at a higher flow rate, which restricted the contact between the chromium ions in the solution and the biosorbent. Thus, at a higher flow rate, the time to breakthrough time is short, whereas, at a lower flow rate, the time taken to reach breakthrough was delayed [Fig. 5(c-d)]. Also, at a higher flow rate, the chromium ions do not have enough time to diffuse into the pores of the biosorbent and they leave the column before equilibrium could be achieved. Hence, the column performance for the chromium biosorption was better at lower flow rates than at higher flow rates [Fig. 6(a-b)].

BDST model fit to the breakthrough data revealed that the variation of the service time with column bed depth is highly linear, thus indicating its validity in describing the chromium sorption in the continuous column operation. The value of the BDST model parameter N_0 indicated that both the sugarcane bagasse and rice husk were highly efficient in the continuous removal of Cr(III) and Cr(VI), respectively, from aqueous solution. Besides the BDST model, the other break-through models tested in this study accurately described the experimental data. However, the Clark model was the most accurate among these models, probably because it involves both the mass transfer and the equilibrium sorption of chromium on to the biosorbents in predicting the breakthrough phenomenon. Overall, this column study proved an excellent potential of both rice husk and sugarcane bagasse as cheaply available agricultural waste materials in the removal of chromium from wastewater.

Mechanism of chromium removal by sugarcane bagasse and rice husk: The Langmuir sorption isotherm, which is probably the best known and most widely applied, supposes a monolayer sorption by physical forces with a homogeneous distribution of sorption sites and sorption energies, without any interaction between the sorbed molecules[33]. Thus, the high values of q_{max} and b obtained for Cr(III) and Cr(VI) biosorption

TABLE-7
DIFFERENT BREAKTHROUGH MODELS TESTED FOR CHROMIUM BIOSORPTION IN THE COLUMN STUDY

Model	Equation	Equation No.	Estimable parameters	Reference
BDST	$t = \frac{ZN_o}{C_oF} - \frac{1}{KC_o}\ln\left(\frac{C_o}{C_B} - 1\right)$	(17)	N_o, K, Z_o	29
Thomas	$\ln\left(\frac{C_o}{C_t} - 1\right) = \frac{k_{TH}q_om}{Q} - k_{TH}C_ot$	(18)	q_o, k_{TH}	35
Yoon-Nelson	$\ln\left(\frac{C_t}{C_o - C_t}\right) = k_{YN}t - \tau k_{YN}$	(19)	k_{YN}, τ	34
Clark	$\ln\left[\left(\frac{C_i}{C_e}\right)^{n-1} - 1\right] = -r't + \ln B$	(20)	r', B	35

TABLE-8
ESTIMATED BREAKTHROUGH MODEL PARAMETERS FOR CHROMIUM BIOSORPTION IN THE COLUMN STUDY

Experimental conditions			Thomas model			Yoon-Nelson model			Clark model		
Z (cm)	Q (mL min^{-1})	C_o (mg L^{-1})	q_o (mg g^{-1})	k_{TH} (mL mg^{-1} min^{-1})	R^2	k_{YN} (mg g^{-1})	τ (h)	R^2	r'	B	R^2
Chromium(III)											
10	10	30	137.5	0.03083	0.9875	0.9251	6.508	0.987	1.683	524394.7	0.945
20	10	30	152.9	0.02201	0.9741	0.6586	9.395	0.986	1.292	5377316.4	0.995
30	10	30	174.3	0.01392	0.9184	0.4814	15.901	0.891	0.968	45262978.3	0.944
10	20	30	252.1	0.03496	0.8983	1.0489	4.614	0.898	1.611	16632.2	0.965
10	30	30	247.2	0.04354	0.9179	1.3063	3.137	0.917	2.000	3901.04	0.975
Chromium(VI)											
10	10	30	204.1	0.02589	0.9869	0.7767	7.355	0.986	1.253	135537.0	0.968
20	10	30	213.7	0.01803	0.979	0.541	12.611	0.979	1.062	6318548.0	0.969
30	10	30	238.2	0.01147	0.9424	0.3443	19.812	0.942	0.690	7897051.3	0.972
10	20	30	441.7	0.02957	0.9721	0.9556	5.624	0.972	1.611	98715.7	0.989
10	30	30	364.4	0.03185	0.9614	0.8872	4.545	0.961	1.493	6876.7	0.982

TABLE-9
ESTIMATED BDST MODEL PARAMETERS FOR CHROMIUM BIOSORPTION IN THE COLUMN STUDY

BDST parameter	Cr(III)		Cr(VI)	
	10 % Saturation	50 % Saturation	10 % Saturation	50 % Saturation
N_o (mg L^{-1})	2292.984	4394.886	2722.9185	4012.722
K (L mg^{-1} h)	0.439357	0.0026937	0.1464816	0.0034514
Z_o (cm)	0.41675	0.65217391	1.0526316	0.4761429
R^2	0.9948	0.9944	0.9918	0.9932

Inlet chromium concentration = 30 mg L^{-1}, particle size = 0.3-0.7 mm, temperature = 25 °C

using sugarcane bagasse and rice husk, respectively, indicated both heavy metal uptake and high affinity between the biosorbent and the chromium ions (Table-3). In contrast to this model, the Freundlich isotherm is originally empirical in nature, but was later interpreted to heterogeneous multilayer adsorption of ions[34]. The high values of the sorption capacity (K_F) and heterogeneity factor (n) obtained using this model further suggested a high affinity of both Cr(III) and Cr(VI) for sugarcane bagasse and rice husk, respectively, in addition to a high distribution of metal binding sites on its surface.

SIPS isotherm at a low metal concentration effectively reduces to Freundlich isotherm when 1/n <<< 1. At a high metal concentration and when 1/n value equals to unity, it predicts a monolayer sorption capacity characteristic of the Langmuir isotherm[32]. In the present study, the values of 1/n greater than 0.5 indicates that the biosorption of Cr(III) and Cr(VI) by sugarcane bagasse and rice husk, respectively, is more of a Langmuir form than that of Freundlich. Similar to the SIPS isotherm model, the Redlich-Peterson isotherm reduces to a linear isotherm in the case of low surface coverage for $\beta = 0$ and to the Langmuir isotherm form when $\beta = 1$. However, Freundlich form is evident at a β value greater than one. The β value obtained in the present study using this isotherm further confirmed that the Cr(VI) biosorption by rice husk follows the Langmuir isotherm. A high K_R value obtained for sugarcane bagasse and rice husk again confirmed the high affinity of Cr(III) and Cr(VI) to sugarcane bagasse and rice husk, respectively.

The removal of Cr(III) and Cr(VI) by sugarcane bagasse and rice husk, respectively, followed the pseudo second-order kinetics model (Table-4), thus indicating a diffusion controlled biosorption process based on chemical reaction, such as that involving ion exchange between the biosorbent and the chromium ions[31].

Conclusion

This study proved that the low-cost available sugarcane bagasse and rice husk were most effective among the six different agricultural wastes as a potential biosorbent for effective removal of chromium from aqueous solution under both the batch and continuous conditions. The chromium removal in the batch was highly dependent on pH, initial chromium concentration, biomass dose and contact time. FTIR analysis of raw and chromium loaded rice husk revealed the participation and presence of -NH, -CH, -COO and -OH groups in the biosorption process. SEM-EDX analyses further confirmed the chromium biosorption on to the biomass. The chromium sorption kinetics by these biosorbents was governed by the intra-particle diffusion mechanism, mainly involving monolayer sorption theory.

Continuous biosorption of Cr(III) and Cr(VI) in the respective columns revealed the feasibility of the process in treating chromium containing wastewater over a long period of continuous operation as it yielded a very high sorption capacity. Whereas an increase in the feed flow rate led to early breakthrough of chromium in the respective columns, an increase in the bed depth led to a prolonged breakthrough time with an increase in the metal uptake capacity. Among the different breakthrough models applied to describe the dynamics of chromium biosorption by sugarcane bagasse and rice husk in their respective columns, the BDST, Yoon-Nelson and Clark models were found to be highly accurate.

ACKNOWLEDGEMENTS

The authors acknowledge with thanks the necessary facilities provided by Centre for the Environment, IIT Guwahati, India, for carrying out this research work. The authors also thank the Department of Chemistry and the Central Instrumentation Facility at IIT Guwahati, India, for FTIR and SEM analyses, respectively.

REFERENCES

1. N.M. Rane, R.S. Sapkal, V.S. Sapkal, M.B. Patil and S.P. Shewale, *Int. J. Chem. Sci.*, **1**, 65 (2010).
2. A. Sahranavard Ahmadpour and M. R. Doosti, *Eur. J. Sci. Res.*, **58**, 392 (2011).
3. S. Chen, Q. Yue, B. Gao, Q. Li, X. Xu and K. Fu, *Bioresour. Technol.*, **113**, 114 (2012).
4. B. Singha and S.K. Das, *Colloids Surf. B*, **84**, 221 (2011).
5. V. Murphy, H. Hughes and P. McLoughlin, *Chemosphere*, **70**, 1128 (2008).
6. Y. Ho, J. Porter and G. McKay, *Water Air Soil Pollut.*, **141**, 1 (2002).
7. N. Bishnoi, R. Kumar, S. Kumar and S. Rani, *J. Hazard. Mater.*, **145**, 142 (2007).
8. D. Onyancha, W. Mavura, J.C. Ngila, P. Ongoma and J. Chacha, *J. Hazard. Mater.*, **158**, 605 (2008).
9. A. Sari and M. Tuzen, *J. Hazard. Mater.*, **160**, 349 (2008).
10. Y. Yun, D. Park, J. Park and B. Volesky, *Environ. Sci. Technol.*, **35**, 4353 (2001).
11. K. Pakshirajan, A.N. Worku, M.A. Acheampong, H.J. Lubberding and P.N.L. Lens, *Appl. Biochem. Biotechnol.*, **170**, 498 (2013).
12. M. Aliabadi, K. Morshedzadeh and H. Soheyli, *Int. J. Environ. Sci. Technol.*, **3**, 321 (2006).
13. M.A. Shouman, N.A. Fathy, S.A. Khedr and A.A. Attia, *Adv. Phys. Chem.*, Article ID 159712 (2013).
14. D. Suman, *Int. J. Environ. Sci. (China)*, **3**, 341 (2012).
15. K. Sbihi, O. Cherifi and M. Bertrand, *Am. J. Sci. Ind. Res. (India)*, **3**, 27 (2012).
16. B. Kavita and H. Keharia, *Int. J. Chem. Eng.*, **1**, 7 (2012).
17. A. Yaqub, M.S. Mughal, A. Adnan, W.A. Khan and K.M. Anjum, *J. Anim. Plant Sci.*, **22**, 408 (2012).
18. M.B. Sciban, J. Prodanovic and R. Razmovski, *Acta Period. Technol.*, **43**, 335 (2012).
19. M.V. Subbaiah, S. Kalyani, G.S. Reddy, V.M. Boddu and A. Krishnaiah, *E-J. Chem.*, **5**, 499 (2008).
20. H. Mosavian and M. Tajee, *Iran. J. Chem. Eng.*, **8**, 11 (2011).
21. S. Mohan and G. Sreelakshmi, *J. Hazard. Mater.*, **153**, 75 (2008).
22. N. Fahim, B. Barsoum, A. Eid and M. Khalil, *J. Hazard. Mater.*, **136**, 303 (2006).
23. A. Sivaprakash, R. Aravindhan, J. Raghavarao and B.N. Nair, *Appl. Ecol. Environ. Res.*, **7**, 45 (2009).
24. P. Srivastava and S.H. Hasan, *BioResource*, **6**, 3656 (2011).
25. R. Elangovan, L. Philip and K. Chandraraj, *J. Hazard. Mater.*, **152**, 100 (2008).
26. G. Blázquez, F. Hernáinz, M. Calero, M.A. Martín-Lara and G. Tenorio, *Chem. Eng. J.*, **148**, 473 (2009).
27. A.K. Bhattacharya, T.K. Naiya, S.N. Mandal and S.K. Das, *Chem. Eng. J.*, **137**, 529 (2008).
28. S. Qaiser, A.R. Saleemi and M. Umar, *J. Hazard. Mater.*, **166**, 998 (2009).
29. M. Jain, V.K. Garg and K. Kadirvelu, *Bioremediat. J.*, **17**, 30 (2013).
30. Z. Xu, J. Cai and B. Pan, *J. Zhejiang Univ. Sci. A*, **14**, 155 (2013).
31. B. Preetha and T. Viruthagiri, *Sep. Purif. Technol.*, **57**, 126, (2007).
32. L.D. Wilson, M.H. Mohamed and C.L. Berhaut, *Materials*, **4**, 1528 (2011).
33. C.E. Borba, R. Guirardello, E.A. Silva, M.T. Veit and C.R.G. Tavares, *Biochem. Eng. J.*, **30**, 184 (2006).
34. P.K. Pandey, S.K. Sharma and S.S. Sambi, *Int. J. Environ. Sci. Technol.*, **7**, 395 (2010).
35. N.V. Medvidovic, J. Peric, M. Trgo and M.N. Muzek, *Micropor. Mesopor. Mater.*, **105**, 298 (2007).